Received: 22 June 2020 | Revised: 14 September 2020 | Accepted: 13 October 2020

IET Control Theory & Applications

DOI: 10.1049/cth2.12063

The Institution of Engineering and Technology WILEY

ORIGINAL RESEARCH PAPER

Analysis and experimental application of a dead-time compensator for input saturated processes with output time-varying delays

Thiago Alves Lima[1,2] | **Sophie Tarbouriech**[2] | **Frédéric Gouaisbaut**[2] | **Magno Prudêncio de Almeida Filho**[1,3] | **Pedro García**[3] | **Bismark Claure Torrico**[1] | **Fabrício Gonzalez Nogueira**[1]

[1] Department of Electrical Engineering, Federal University of Ceará, Fortaleza, Brazil

[2] LAAS-CNRS, Université de Toulouse, CNRS, Toulouse, France

[3] Instituto de Automática e Informática Industrial, Universitat Politécnica de Valéncia, Valéncia, Spain

Correspondence
Thiago Alves Lima, Department of Electrical Engineering, Federal University of Ceará, Fortaleza, Brazil.
Email: thiago.lima@alu.ufc.br

Funding information
Coordenação de Aperfeiçoamento de Pessoal de Nível Superior, Grant/Award Number: 001; Agence Nationale de la Recherche, Grant/Award Number: 18-CE40-0010

Abstract

Dead-time compensators (DTCs) are a family of classical controllers derived from the Smith Predictor. Their main characteristic is that they explicitly employ the model of the open-loop process to feedback a predicted value of the non-delayed system, thus obtaining *compensation* of the delay. Such a perfect compensation is not achievable in the case of time-varying delays. This paper addresses stability analysis of a DTC structure in this situation, in addition to considering saturating actuators and disturbances of limited energy. Specific challenges related to the DTC closed loop are taken into account in the developed theoretical conditions, which are expressed in terms of linear matrix inequalities by using an adequate Lyapunov–Krasovskii functional and generalised sector conditions. Furthermore, a new approach for the definition of the set of initial conditions in an augmented space in conjunction with the Lyapunov–Krasovskii functional is presented. Besides theoretical innovations, practical discussion about the relation between the tuning of DTC controllers and robustness for this class of systems is presented through numerical examples. An experimental application on a neonatal incubator prototype is carried out to emphasise the effectiveness of the results.

1 | INTRODUCTION

Time delay, which appears in many industrial processes, is a challenging issue in the process control area since the transport delay can lead the system to undesired oscillatory closed-loop response or even instability [1]. According to [2, 3], the stability analysis and the robust control of time-delay systems are also of theoretical importance since it belongs to the wide class of infinite-dimensional systems (in the continuous-time case), which are not so easy to handle theoretically.

Besides time delay, another major topic in control systems is actuator saturation [4, 5]. Most variables in industrial processes work near or at their maximum and minimum limits in order to optimise production. The nonlinear nature of the closed loop can also lead to instability. Therefore, such constraints must be taken into account during closed-loop stability analysis prior to the controller practical implementation. The presence of isolated non-linearities, as the actuator saturation, is yet an active topic of research (see for example, [6–8]). The problem of sensor saturation has also recently been studied in [9, 10].

Regarding time delays, the so-called dead-time compensators (DTCs) have been widely studied over the years due to their ability to improve the performance and robustness of the closed-loop system for processes with constant input or output time delay [1]. The first DTC was proposed in [11], also known in the literature as the Smith predictor (SP). Since then, several extensions have been proposed to deal with stable, unstable, and integrative processes, and to improve robustness, disturbance rejection, and measurement noise attenuation [12]. Some recent works intended to improve these characteristics can be found in [13–17], among others. Other solutions not involving the classical DTCs have also been proposed in recent years; for example,

in [18], the adaptive control of a class of time-varying non-linear systems with constant delay is investigated. The robust control of non-linear systems with constant delays was also explored in [19]. In [20], tuning rules for low-order controllers (including proportional-integral-derivative (PID) controllers) are revisited and the robust control of time-delayed single-input single-output (SISO) is addressed.

Nonetheless, due to the growing importance of Networked Control Systems (NCSs) [21–23], the problem of time-varying delays started to gain more importance in the recent years when compared to the case of constant delays (even if the constant delay is uncertain). To cite a few works, the stability of structures for the control of time-varying delay systems has recently been studied along the problems of linear time-varying (LTV) processes [24], non-linear systems [25], non-minimum phase systems [26], and mismatched disturbances [27]. In this case, the traditional DTC will no longer be able to provide perfect compensation of the delay, that is, will not be able to eliminate the delay from the feedback loop, which is its main characteristic. Due to this problem, the work in [28] develops stability analysis of the Filtered Smith Predictor (FSP) for the case of time-varying delay processes in order to evaluate the FSP ability to deal with this case. However, saturating actuators, which is common in practical applications and places an undesired non-linearity in the closed-loop system, has not been considered in the aforementioned work.

Concerning the classical DTCs, in [1], it is argued that one strategy to take the saturation into account in DTC structures is to include the model of the saturation at the input of the model of the plant. As highlighted by the authors, the fundamental property of the Smith Predictor still holds in this situation: the dead time is eliminated from the main feedback loop in the case of no modelling errors and no disturbances. However, time-varying delays are not considered and a formal stability analysis with the characterisation of a set of initial conditions and/or disturbances for which the internal stability of the closed loop is preserved is not presented by the authors. In [29], a practical solution for the control of systems with constant delay and input saturation is presented based on the design of a DTC for the linear system plus the addition of anti-windup to deal with saturation aspects. Nevertheless, a procedure for estimating the region of attraction in the case of uncertain (or time-varying) delays is not presented either.

In the current paper, we revisit the DTC structure to provide theoretical conditions, expressed through linear matrix inequalities (LMIs), for the stability analysis of the closed loop considering systems with both input saturation and output time-varying delays. One of the objectives is to characterise the region of admissible initial conditions for which the closed-loop stability is ensured despite the presence of saturating input. To do this, we consider an adequate Lyapunov–Krasovskii functional (LKF) and generalised sector conditions. Additionally, we aim at using the analysis to relate the tuning of DTCs with both robustness and performance of the closed loop. Although seminal works addressing the joint problems of time delays and input saturation can be found in the literature [30–33], fundamental differences can be cited: (i) All of them consider state delays, while we consider output delays, a different kind of delay present in numerous applications, as in chemical reaction processes. (ii) All of them are in continuous-time since they do not deal with model-based controls. On the other hand, we propose the use of DTCs, which are high-order predictive controllers employing the model of the process and that have been frequently used in practical applications in the last decades. Since all strategies employing the plant model for the control of time-delay systems need to be, in practice, digitally implemented, we work in the discrete-time domain which is more realistic in this case. (iii) Neither of them deals with time-varying delays, which appear in many real applications and are more difficult to treat in a theoretical point of view. Additionally, this paper proposes a new methodology for the estimate on the region of stability along with LKFs which can lead to less conservative results than those commonly used (see Sections 2.3 and 4.1). Such a novel methodology can be applied in any work using LKFs for the stability of discrete-time time-delayed systems and is, therefore, a technical contribution not necessarily linked with the DTC controller.

The paper is organised as follows: Section 2 describes the complete system under consideration, the involved contributions, and states the mathematical problem we intend to solve. Section 3 is dedicated to some preliminary results. In Section 4, the main results are presented. Section 5 brings simulation results of the DTC, followed by the experimental application in Section 6. Finally, concluding remarks are brought in the last section of the paper.

Notation. For a matrix $Y \in \mathbb{R}^{n\times m}$, $Y^\top \in \mathbb{R}^{m\times n}$ means its transpose, $Y_{(i)}$ denotes its ith row, while for $v \in \mathbb{R}^m$, $v_{(i)}$ denotes its ith component. For matrices $W = W^\top \in \mathbb{R}^{n\times n}$ and $Z = Z^\top \in \mathbb{R}^{n\times n}$, $W > Z$ means that $W - Z$ is positive definite. Likewise, $W \geq Z$ means that $W - Z$ is positive semi-definite. $\mathbb{S}_n^+$ stands for the set of positive definite matrices. I and 0 denote identity and null matrices of appropriate dimensions, although their dimensions can be explicitly presented whenever relevant. In this case, $0_{n\times m}$ represents the $n \times m$ null matrix, while I_n represents $n \times n$ identity matrix. The $\star$ in $\begin{bmatrix} A & B \\ \star & C \end{bmatrix}$ denotes symmetric blocks, that is $\star = B^\top$. Finally, for matrices W and Z, diag(W, Z) corresponds to the block-diagonal matrix.

2 | PROBLEM FORMULATION

2.1 | General view

In the paper, we consider a discrete-time system controlled by a DTC and subject to input saturation. The structure is depicted in Figure 1 constituted by a plant $\mathcal{P}$, a reference filter $\mathcal{F}_0$, subsystem $\mathcal{S}$ and a filter $\mathcal{F}_r$. In this paper, we consider

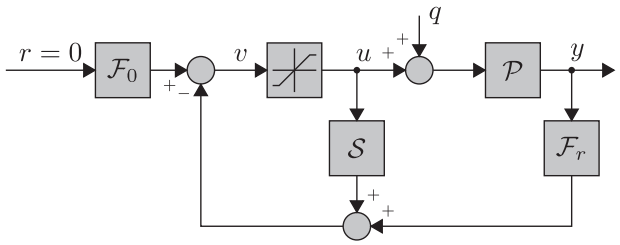

FIGURE 1 DTC controller implementation scheme

the regulatory case, with reference $r = 0$, and the DTC controller from [16]. However, the developed LMIs can easily be applied to other variations of the Filtered Smith Predictor. The complete system under consideration issued from the connection of the plant, the system $\mathcal{S}$, and the filter $\mathcal{F}_r$ is described as follows:

$$\mathcal{P} \triangleq \begin{cases} x_{p_{k+1}} = \mathrm{A}_p x_{p_k} + \mathrm{B}_p(u_k + q_k) \\ y_k = \mathrm{C}_p x_{p_{k-d_k}}, \end{cases} \tag{1}$$

$$\mathcal{S} \triangleq \begin{cases} x_{s_{k+1}} = \mathrm{A}_s x_{s_k} + \mathrm{B}_s u_k \\ y_{s_k} = \mathrm{C}_s x_{s_k}, \end{cases} \tag{2}$$

$$\mathcal{F}_r \triangleq \begin{cases} x_{f_{k+1}} = \mathrm{A}_f x_{f_k} + \mathrm{B}_f y_k \\ y_{f_k} = \mathrm{C}_f x_{f_k} + \mathrm{D}_f y_k, \end{cases} \tag{3}$$

where $x_{p_k} \in \mathbb{R}^{n_p}$ is the plant state vector, $x_{s_k} \in \mathbb{R}^{n_s}$ is the state of $\mathcal{S}$, and $x_{f_k} \in \mathbb{R}^{n_f}$ is the state of $\mathcal{F}_r$. $y_k \in \mathbb{R}$ is the measured output and $u_k \in \mathbb{R}$ is the control input, while $y_{s_k} \in \mathbb{R}$ and $y_{f_k} \in \mathbb{R}$ are the outputs of $\mathcal{S}$ and $\mathcal{F}_r$, respectively. Matrices A_p, B_p, and C_p are all constant, known, and of appropriate dimensions. The plant output delay is bounded and time-varying such as $1 \leq d_m \leq d_k \leq d_\mathrm{M}$, and can arbitrarily vary within such limits. Integers d_m and d_M are known, whereas the value of d_k at each sampling time is unknown. Additionally, the plant is subject to an input disturbance q_k which supposedly belongs to the following set of functions

$$\mathcal{Q} = \left\{ q_k : \mathbb{R}^+ \mapsto \mathbb{R}; \sum_{k=0}^{\infty} q_k^\top q_k \leq \delta \right\}, \tag{4}$$

where $\delta > 0$ represents a bound on the signal energy of q_k. The connection between $\mathcal{P}$, $\mathcal{S}$ and $\mathcal{F}_r$ is realised by

$$\begin{aligned} u_k &= sat(v_k) \\ v_k &= -y_{s_k} - y_{f_k}, \end{aligned} \tag{5}$$

where the saturation is classically defined as

$$sat(v_k) = sign(v_k) \times min\{|v_k|, \bar{u}\}, \bar{u} > 0, \tag{6}$$

$\bar{u}$ being the level of saturation.

Then, the closed-loop system (1), (2), (3) and (5) reads:

$$\begin{cases} x_{k+1} = \mathrm{A}x_k + \mathrm{A}_\mathrm{d} x_{k-d_k} + \mathrm{B}sat(v_k) + \mathrm{B}_q q_k \\ v_k = \mathrm{K}x_k + \mathrm{K}_\mathrm{d} x_{k-d_k} \\ x_k = \phi_k, \ k \in [-d_\mathrm{M}, 0] \\ y_k = \mathrm{C}x_{k-d_k} \end{cases} \tag{7}$$

with

$$\mathrm{A} = \begin{bmatrix} \mathrm{A}_p & 0 & 0 \\ 0 & \mathrm{A}_s & 0 \\ 0 & 0 & \mathrm{A}_f \end{bmatrix}, \mathrm{A}_\mathrm{d} = \begin{bmatrix} 0 & 0\,0 \\ 0 & 0\,0 \\ \mathrm{B}_f \mathrm{C}_p & 0\,0 \end{bmatrix},$$

$$\begin{bmatrix} \mathrm{K} \\ \mathrm{K}_\mathrm{d} \\ \mathrm{C} \end{bmatrix} = \begin{bmatrix} 0 & -\mathrm{C}_s & -\mathrm{C}_f \\ -\mathrm{D}_f \mathrm{C}_p & 0 & 0 \\ \mathrm{C}_p & 0 & 0 \end{bmatrix}, \begin{bmatrix} \mathrm{B}\ \mathrm{B}_q \end{bmatrix} = \begin{bmatrix} \mathrm{B}_p \mathrm{B}_p \\ \mathrm{B}_s\ 0 \\ 0\ 0 \end{bmatrix},$$

where $x_k = \begin{bmatrix} x_{p_k}^\top & x_{s_k}^\top & x_{f_k}^\top \end{bmatrix}^\top \in \mathbb{R}^n$, $n = n_p + n_s + n_f$, and ϕ_k is the initial condition at the interval $[-d_\mathrm{M}, 0]$.

Remark 1. There is no loss of generality in considering the regulatory case, since industrial processes can be modelled around an operation point, and a simple change of variables can transform the desired output in zero.

2.2 | Notes on the controller design

The controller matrices A_s, B_s, C_s, A_f, B_f, C_f and D_f have been designed following the steps in [16], that is, to establish a desired response of the nominal linear system. In other words, the controller design considered that the time delay d_k was constant $d_k = d_n$, and the non-occurrence of the saturation. Since the objective of this paper is not the controller design, but rather closed-loop stability analysis, we just briefly review some properties of the controller. The computation of $\mathcal{S}$ depends on the process model with nominal delay d_n[1], the desired $2n_p - 1$ closed-loop poles, and the robustness filter $\mathcal{F}_r$. Furthermore, $\mathcal{S}$ provides perfect delay compensation for the nominal case, that is, nominal delay and no input saturation. The robustness filter $\mathcal{F}_r$ should be designed to guarantee an internally stable implementation structure (A_f and A_s must be Schur stable matrices), to make the equivalent controller have integral action, and to establish a desired compromise between robustness and disturbance rejection.

The state matrix A_f can be defined as $\mathrm{A}_f = \rho \mathrm{I}_{n_p+1}$, where $0 < \rho < 1$ is the robustness filter tuning parameter. In the linear time-invariant (LTI) case, by setting higher values of ρ, one can increase the robustness of the system to modelling uncertainties, while smaller values of ρ speedup the disturbance rejection response. More details on the design and tuning of DTC structures for LTI systems can be found in its vast literature [15, 28].

[1] The nominal delay d_n is defined as the rounding to the nearest integer of $(d_m + d_\mathrm{M})/2$.

Remark 2. In DTC structures, the choice of ρ is essential, being its most important tuning parameter. Also, although ρ designates the robustness filter $\mathcal{F}_r$ poles, its value directly influences almost all of the other controller matrices (A_s, C_s, B_f, C_f, D_f), which hampers the development of LMI based stabilisation of the whole system due to the difficulty to deal with non-linearities. This will be subject of a succeeding work.

2.3 | More details on the formulation and contributions

Although the open-loop process (1) has output delay, the closed-loop system representation (7) is in the form of a state-delayed discrete-time system with control saturation. Many works can be cited regarding the continuous counterpart of this kind of system [34–36]. Fewer are dedicated to the discrete-time case; however, one can cite [37], [38], and most recently [39], which deals with the linear parameter varying (LPV) case. Besides dealing with the LPV case, it is important to highlight other differences from the formulation in this work. First of all, the control law in [39] does not deal with the NCS case where the delay appears in the plant output rather than in the plant state. Furthermore, the formulation proposed in [39] implements a control law that assumes knowledge of the full history of the plant state, that is the extended state $\overline{x_{p_k}} = \left[x_{p_k}^\top \; x_{p_{k-1}}^\top \; \cdots \; x_{p_{k-d_M}}^\top\right]^\top$, and its closed-loop representation does not contain the term $K_d x_{k-d_k}$ since it would require knowledge of the value d_k at each sampling time. This is not the case in this work since the actual implemented control law only requires knowledge/measurement of the output y_k, and thus the control v_k in (7) is just the equivalent system for analysis.

It is also interesting to comment that, although works in this area usually employ LKFs, [39] uses the approach of augmented Lyapunov. As highlighted by the authors therein, the main drawback of the works based in the Lyapunov–Krasovskii approach is that all of them characterise the region of attraction based on the norm of the sequence of initial conditions, which often leads to conservative estimates. In order to deal with this problem, in [39], the estimate on the region of attraction is characterised in an augmented space, which is convenient by means of the use of the augmented functional approach.

One of the theoretical innovation in this work comes from a mix between the ideas above. When dealing with DTC structures, it is necessary to keep in mind the problem of high order dimensions of the closed loop, which increases proportionally to the nominal delay d_n and the plant order n_p. The total order of the closed loop (7) is given by $n = n_p + n_s + n_f$, with $n_f = n_p + 1$, $n_s = n_f + d_n$, resulting in $n = 3n_p + d_n + 2$. As DTCs are usually applied to control systems with big delays (where conventional controllers such as PID and feedback gains alone are not as effective), the LMI conditions should, ideally, have a low number of decision variables to avoid tractability problems due to the high dimensionality of (7). Due to that, the augmented functional approach of [39] is not practical and can lead to high numerical complexity. On the other hand, differently from the works based on LKFs, we define the initial conditions in an augmented space, avoiding the conservatism linked with the norm of the sequence approach therein.

On the practical side, we apply the developed conditions to link the DTC tuning variable ρ with the system robustness. The specific challenges related to the DTC closed loop are taken into account in the developed theoretical conditions, and the relation between the tuning of DTCs and the robustness of the closed loop is established. To the best of the authors' knowledge, no work in the literature of DTC has done that for the case of both time-varying delays and saturation. The experimental application considering both these conditions is also unprecedented.

2.4 | Problem statement

The central objective with respect to system (7) can then be summarised as follows:

Problem 1. Given a process model defined by A_p, B_p, C_p and the nominal delay d_n, the controller matrices A_s, B_s, C_s, A_f, B_f, C_f, and D_f, provide LMI-based stability analysis in the case of simultaneous output time-varying delays and control saturation. More specifically, one aims at providing adequate conditions to estimate:

(i) The size of sets of guaranteed asymptotic stability for the closed loop.
(ii) The energy bound on the external disturbance belonging to the set $\mathcal{Q}$.
(iii) Lower and upper bounds on the time-varying delay.

Then, by means of numerical examples, one aims at using the solution to Problem 1 to relate the DTC tuning parameter ρ to items (i), (ii) and (iii).

3 | PRELIMINARY RESULTS

In general, the stability of time-delayed systems can be tackled by using either delay-independent or delay-dependent conditions [2]. The latter case (in which bounds on the delay are explicitly considered) is adopted in this work. The problem of providing stability guarantees for systems with delayed states can be solved by choosing an appropriate Lyapunov functional V_k and its consequent manipulation, which can lead to more or less conservative results. In recent years, many works have been dedicated to the construction of such Lyapunov functionals. All these methods are relying on an appropriate choice of a LKF, and the way to upper bound some sums. Recently, many researchers have been dedicated to the goal of decreasing the conservatism inherent of these upper-bounds by discovering new inequalities. For more details, see the works

of [40–46]. However, this paper chooses to use the classical Jensen's inequality [47], which in combination with the use of Finsler's Lemma and the reciprocally convex approach [48] can potentially yield a good compromise between numerical complexity and the level of conservatism of the developed condition, as it will be shown later. Although the use of more complex inequalities could be interesting, it will be done in the future.

3.1 | Auxiliary lemmas

In the development of our conditions, we apply Finsler's Lemma [49], the discrete-time version of the Jensen's inequality, taken from [44, 47], and the reciprocally convex approach [3, 48], stated in the following three Lemmas.

Lemma 1. *[49] Consider $\gamma \in \mathbb{R}^n$, $\Upsilon = \Upsilon^\top \in \mathbb{R}^{n\times n}$, and $\Gamma \in \mathbb{R}^{m\times n}$. The following facts are equivalent:*

i) $\gamma^\top \Upsilon \gamma < 0$, $\forall \gamma$ *such that* $\Gamma\gamma = 0$, $\gamma \neq 0$.
ii) ${\Gamma^\perp}^\top \Upsilon \Gamma^\perp \prec 0$, *where* $\Gamma\Gamma^\perp = 0$.
iii) $\exists \mathrm{J} \in \mathbb{R}^{n\times m}$ *such that* $\Upsilon + \mathrm{J}\Gamma + \Gamma^\top \mathrm{J}^\top \prec 0$.

Lemma 2. *[44, 47] For integers $a < b$, a function $f : \mathbb{Z}[a, b] \to \mathbb{R}^n$ and a matrix $\mathrm{R} \succ 0$, the following inequality holds*

$$\sum_{k=a}^{b} f_k^\top \mathrm{R} f_k \geq \frac{1}{l}\left(\sum_{k=a}^{b} f_k^\top\right)\mathrm{R}\left(\sum_{k=a}^{b} f_k\right), \tag{8}$$

where $l = b - a + 1$ denotes the length of interval $[a, b]$ in $\mathbb{Z}$.

Lemma 3. *[3, 48] For given positive integers n, m, a scalar $\alpha \in (0, 1)$, a matrix R_1 in $\mathbb{S}_n^+$ and two matrices W_1, W_2 in $\mathbb{R}^{n\times m}$. Define, for all vector $\zeta \in \mathbb{R}^m$, the function $\Theta(\alpha, \mathrm{R})$ given by:*

$$\Theta(\alpha, \mathrm{R}_1) = \frac{1}{\alpha}\zeta^\top \mathrm{W}_1^\top \mathrm{R}_1 \mathrm{W}_1 \zeta + \frac{1}{1-\alpha}\zeta^\top \mathrm{W}_2^\top \mathrm{R}_1 \mathrm{W}_2 \zeta.$$

If there exists $\mathrm{U}_{12} \in \mathbb{R}^{n\times n}$ such that $\begin{bmatrix} \mathrm{R}_1 & \mathrm{U}_{12} \\ \star & \mathrm{R}_1 \end{bmatrix} \geq 0$, then the following inequality holds

$$\min_{\alpha\in(0,1)} \Theta(\alpha, \mathrm{R}) \geq \begin{bmatrix} \mathrm{W}_1\zeta \\ \mathrm{W}_2\zeta \end{bmatrix}^\top \begin{bmatrix} \mathrm{R}_1 & \mathrm{U}_{12} \\ \star & \mathrm{R}_1 \end{bmatrix} \begin{bmatrix} \mathrm{W}_1\zeta \\ \mathrm{W}_2\zeta \end{bmatrix}.$$

3.2 | Stability in the unsaturated case

We initially develop results for the unsaturated case (i.e. $u_k = v_k$) with no disturbance ($q_k = 0$). This is an important step in order to check if the trade-off between the numerical complexity of the condition and the obtained results is well balanced. Especially, the ideal scenario for analysis of DTCs is to obtain conditions that have fewer decision variables and work well with higher delays. Also, some of the content of the proof in this section will be used in the main results in Section 4. The developed conditions will be tested in a benchmark example from the literature.

The simplified version of (7) by taking into account the connection $u_k = v_k$, and $q_k = 0$, is given by:

$$\begin{cases} x_{k+1} = \mathbb{A}x_k + \mathbb{A}_\mathrm{d} x_{k-d_k} \\ x_k = \phi_k, \ k \in [-d_\mathrm{M}, 0], \end{cases} \tag{9}$$

where $1 \leq d_m \leq d_k \leq d_\mathrm{M}$, $x_k \in \mathbb{R}^n$, ϕ_k is the initial condition at the interval $[-d_\mathrm{M}, 0]$, $\mathbb{A} = \mathrm{A} + \mathrm{BK}$, and $\mathbb{A}_\mathrm{d} = \mathrm{A}_\mathrm{d} + \mathrm{BK}_\mathrm{d}$. The system (9) has the same format of those studied in [43, 50], for example. The following theorem establishes a sufficient condition to prove stability of system (9).

Theorem 1. *Consider $d_\Delta = d_\mathrm{M} - d_m$, and assume the existence of matrices Q, R, U, R_1, U_1 in $\mathbb{S}_n^+$, and matrix U_{12} in $\mathbb{R}^{n\times n}$ such that:*

$$\mathrm{T} = \begin{bmatrix} \mathrm{R}_1 & \mathrm{U}_{12} \\ \star & \mathrm{R}_1 \end{bmatrix} \geq 0, \quad {\Gamma^\perp}^\top \Upsilon \Gamma^\perp \prec 0, \tag{10}$$

where $\Gamma^\perp = \begin{bmatrix} \mathbb{A} & 0 & 0 & \mathbb{A}_\mathrm{d} \\ & & \mathrm{I}_{4n} & \end{bmatrix}$ *and*

$$\Upsilon = \begin{bmatrix} \Upsilon_{11} & \Upsilon_{12} & 0 & 0 & 0 \\ \star & \Upsilon_{22} & \mathrm{R} & 0 & 0 \\ \star & \star & \Upsilon_{33} & \mathrm{U}_{12} & \mathrm{R}_1 - \mathrm{U}_{12} \\ \star & \star & \star & -\mathrm{U}_1 - \mathrm{R}_1 & \mathrm{R}_1 - \mathrm{U}_{12}^\top \\ \star & \star & \star & \star & \Upsilon_{55} \end{bmatrix},$$

with

$$\begin{aligned} \Upsilon_{11} &= \mathrm{Q} + \mathrm{R}d_m^2 + \mathrm{R}_1 d_\Delta^2, \\ \Upsilon_{12} &= -\mathrm{R}d_m^2 - \mathrm{R}_1 d_\Delta^2, \\ \Upsilon_{22} &= \mathrm{R}d_m^2 - \mathrm{R} + \mathrm{R}_1 d_\Delta^2 - \mathrm{Q} + \mathrm{U}, \\ \Upsilon_{33} &= \mathrm{U}_1 - \mathrm{R}_1 - \mathrm{R} - \mathrm{U}, \\ \Upsilon_{55} &= \mathrm{U}_{12} + \mathrm{U}_{12}^\top - 2\mathrm{R}_1. \end{aligned}$$

Then system (9) is asymptotically stable for any time-varying delay $d_m \leq d_k \leq d_\mathrm{M}$.

Proof. Consider the following LKF from [2], which is the discrete-time counterpart of the functional used for continuous-time systems in [53]:

$$\mathrm{V}_k = \mathrm{V}_{\mathrm{Q}_k} + \mathrm{V}_{\mathrm{R}_k} + \mathrm{V}_{\mathrm{U}_k} + \mathrm{V}_{\mathrm{U}_{1_k}} + \mathrm{V}_{\mathrm{R}_{1_k}}, \tag{11}$$

with

$$\mathrm{V}_{\mathrm{Q}_k} = x_k^\top \mathrm{Q} x_k,$$

$$\mathrm{V}_{\mathrm{R}_k} = d_m \sum_{m=-d_m}^{-1} \sum_{j=k+m}^{k-1} \eta_j^\top \mathrm{R} \eta_j,$$

$$\mathrm{V}_{\mathrm{U}_k} = \sum_{j=k-d_m}^{k-1} x_j^\top \mathrm{U} x_j,$$

$$\mathrm{V}_{\mathrm{U}_{1_k}} = \sum_{j=k-d_{\mathrm{M}}}^{k-d_m-1} x_j^\top \mathrm{U}_1 x_j,$$

$$\mathrm{V}_{\mathrm{R}_{1_k}} = d_\Delta \sum_{m=-d_{\mathrm{M}}}^{-d_m-1} \sum_{j=k+m}^{k-1} \eta_j^\top \mathrm{R}_1 \eta_j,$$

where $\eta_j = x_{j+1} - x_j$ and $\mathrm{Q}, \mathrm{U}, \mathrm{R}, \mathrm{U}_1$, and R_1 are matrices in $\mathbb{S}_n^+$. Evaluating $\Delta \mathrm{V}_k = \mathrm{V}_{k+1} - \mathrm{V}_k$ along the trajectories of (9), one gets

$$\Delta \mathrm{V}_{\mathrm{Q}_k} = x_{k+1}^\top \mathrm{Q} x_{k+1} - x_k^\top \mathrm{Q} x_k, \tag{12}$$

$$\Delta \mathrm{V}_{\mathrm{R}_k} = d_m^2 \eta_k^\top \mathrm{R} \eta_k - d_m \sum_{j=k-d_m}^{k-1} \eta_j^\top \mathrm{R} \eta_j, \tag{13}$$

$$\Delta \mathrm{V}_{\mathrm{U}_k} = x_k^\top \mathrm{U} x_k - x_{k-d_m}^\top \mathrm{U} x_{k-d_m}, \tag{14}$$

$$\Delta \mathrm{V}_{\mathrm{U}_{1_k}} = x_{k-d_m}^\top \mathrm{U}_1 x_{k-d_m} - x_{k-d_{\mathrm{M}}}^\top \mathrm{U}_1 x_{k-d_{\mathrm{M}}}, \tag{15}$$

$$\Delta \mathrm{V}_{\mathrm{R}_{1_k}} = d_\Delta^2 \left(\eta_k^\top \mathrm{R}_1 \eta_k - \sum_{j=k-d_{\mathrm{M}}}^{k-d_m-1} \frac{\eta_j^\top \mathrm{R}_1 \eta_j}{d_\Delta} \right). \tag{16}$$

By applying Lemma 2 to the summation term in the right-hand side of equation (13) we obtain the bound

$$\Delta \mathrm{V}_{\mathrm{R}_k} \leq \begin{bmatrix} x_{k+1} \\ x_k \\ x_{k-d_m} \end{bmatrix}^\top \begin{bmatrix} \mathrm{R} d_m^2 & -\mathrm{R} d_m^2 & 0 \\ \star & \mathrm{R} d_m^2 - \mathrm{R} & \mathrm{R} \\ \star & \star & -\mathrm{R} \end{bmatrix} \begin{bmatrix} x_{k+1} \\ x_k \\ x_{k-d_m} \end{bmatrix}. \tag{17}$$

To deal with the summation term in (16), first note that it can be split in two parts, one gathering terms in the interval $k - d_k$ to $k - d_m - 1$ and the second between $k - d_{\mathrm{M}}$ and $k - d_k - 1$. Then, apply Lemma 2 to get $d_\Delta \sum_{j=k-d_k}^{k-d_m-1} \eta_j^\top \mathrm{R}_1 \eta_j \geq \mathbb{H}_1$ and $d_\Delta \sum_{j=k-d_{\mathrm{M}}}^{k-d_k-1} \eta_j^\top \mathrm{R}_1 \eta_j \geq \mathbb{H}_2$, where

$$\mathbb{H}_1 = \frac{d_\Delta}{d_k - d_m} \left(x_{k-d_m}^\top - x_{k-d_k}^\top \right) \mathrm{R}_1 \left(x_{k-d_m} - x_{k-d_k} \right),$$

$$\mathbb{H}_2 = \frac{d_\Delta}{d_{\mathrm{M}} - d_k} \left(x_{k-d_k}^\top - x_{k-d_{\mathrm{M}}}^\top \right) \mathrm{R}_1 \left(x_{k-d_k} - x_{k-d_{\mathrm{M}}} \right).$$

TABLE 1 Admissible upper bound d_{M} for various d_m applying Theorem 1; other results from the literature come from Table 1 in [51]

Methods	$d_m =$	2	4	6	7	10	15	20	25	30	No. of variables
Theorem 1		17	17	17	18	20	23	27	31	35	$3.5n^2 + 2.5n$
Proposition 1 [41]		17	17	18	18	20	23	27	31	35	$8n^2 + 3n$
Theorem 2 [52]		22	22	22	22	23	25	28	32	36	$27n^2 + 9n$
Theorem 5 [43]		20	21	21	22	23	25	29	32	36	$10.5n^2 + 3.5n$
Theorem 7 [44]		20	21	21	22	23	25	29	32	36	$20n^2 + 5n$

Consider then Lemma 3 with $\Theta(\alpha, \mathrm{R}_1) = \mathbb{H}_1 + \mathbb{H}_2$, $\alpha = \frac{d_k - d_m}{d_\Delta}$, $\zeta_k = \begin{bmatrix} x_{k-d_m}^\top & x_{k-d_{\mathrm{M}}}^\top & x_{k-d_k}^\top \end{bmatrix}^\top$, $\mathrm{W}_1 = \begin{bmatrix} \mathrm{I} & 0 & -\mathrm{I} \end{bmatrix}$, $\mathrm{W}_2 = \begin{bmatrix} 0 & -\mathrm{I} & \mathrm{I} \end{bmatrix}$ to obtain $\mathbb{H}_1 + \mathbb{H}_2 \geq \chi_k^\top \mathrm{T} \chi_k$, where

$$\chi_k = \begin{bmatrix} x_{k-d_m} - x_{k-d_k} \\ x_{k-d_k} - x_{k-d_{\mathrm{M}}} \end{bmatrix}, \text{ and } \mathrm{T} = \begin{bmatrix} \mathrm{R}_1 & \mathrm{U}_{12} \\ \star & \mathrm{R}_1 \end{bmatrix} \geq 0,$$

for some full matrix U_{12}, leading to:

$$\Delta \mathrm{V}_{\mathrm{R}_{1_k}} \leq d_\Delta^2 \left(x_{k+1}^\top - x_k^\top \right) \mathrm{R}_1 \left(x_{k+1} - x_k \right) - \chi_k^\top \mathrm{T} \chi_k. \tag{18}$$

Adding (12), (14), (15), (17), and (18), and considering extended vector $\gamma_k = \begin{bmatrix} x_{k+1}^\top & x_k^\top & x_{k-d_m}^\top & x_{k-d_{\mathrm{M}}}^\top & x_{k-d_k}^\top \end{bmatrix}^\top$, we obtain the bound $\Delta \mathrm{V}_k \leq \gamma_k^\top \Upsilon \gamma_k$, $\forall \gamma$ such that $\Gamma \gamma = 0$, $\gamma \neq 0$, with $\Gamma = \begin{bmatrix} -\mathrm{I} & \mathbb{A} & 0 & 0 & \mathbb{A}_{\mathrm{d}} \end{bmatrix}$. Thus, by guaranteeing that $\gamma_k^\top \Upsilon \gamma_k < 0$, we ensure that $\Delta \mathrm{V}_k < 0$ and the asymptotically stability of system (9). By application of Lemma 1, this holds if $\Gamma^{\perp^\top} \Upsilon \Gamma^\perp \prec 0$, where $\Gamma^\perp$ is a basis for the null space of Γ, thus completing the proof of Theorem 1. □

Remark 3. The condition in Theorem 1 could also be obtained by means of the equivalent form (iii) of Lemma 1. However, this would lead to an increase of $5n^2$ in the total number of decision variables. In fact, the use of (iii) is more advantageous in case of controller synthesis, due to the flexibility to choose special forms for the Lagrange multiplier J.

3.3 | Benchmark test of Theorem 1

In order to understand the level of conservatism of the conditions in Theorem 1, an example usually employed in the literature is recovered. Consider system (9) with:

$$\mathbb{A} = \begin{bmatrix} 0.8 & 0.0 \\ 0.05 & 0.9 \end{bmatrix}, \quad \mathbb{A}_{\mathrm{d}} = \begin{bmatrix} -0.1 & 0.0 \\ -0.2 & -0.1 \end{bmatrix}.$$

Table 1 shows the obtained results in comparison with others from the literature (see Table 1 in [51]). Although there is a

clear disadvantage in the results for lower bounds on the minimum delay $d_m \leq 10$, we can see an interesting improvement as it becomes higher. As a matter of fact, the obtained results are very close to the best obtained for delays with lower bound $d_m \geq 25$. Also, note that the numerical complexity of the condition is much lower than that of most of the other approaches. This is very important since DTCs are frequently applied to systems with big delay, and the order of the closed loop depends on it, with $n = 3n_p + d_n + 2$, as highlighted earlier in the paper. For comparison, for a process model with $n_p = 2$ and $d_n = 4$, the number of variables of the second condition with least variables [41] is 122% higher than the approach here, and the number of variables in [52] is 648% higher. This is a huge difference that could impact the numerical performance of the conditions. Therefore, we conclude that the choice of LKF and its manipulation has been adequate for the DTC problem in this paper, although it can be improved in future research. In the next section, we use this LKF in conjunction with a generalised sector condition to provide stability analysis to system (7).

4 | MAIN RESULTS

In this section, we present stability analysis conditions for the saturated closed-loop system (7). Theoretical preliminaries are initially reviewed, including the generalised sector condition and the definition of a set of initial conditions for which stability guarantees will be inspected.

4.1 | Theoretical preliminaries

Consider the deadzone non-linearity φ, defined as follows

$$\varphi(v_k) = v_k - sat(v_k), \tag{19}$$

and the following set

$$\mathscr{L}(v - \theta, \overline{u}) = \{v \in \mathbb{R}; \theta \in \mathbb{R}; -\overline{u} \leq v - \theta \leq \overline{u}\}. \tag{20}$$

We then recall the following result which was introduced in [54], here adapted for the simpler case of systems with a one-dimensional control input.

Lemma 4. *[Generalised sector condition] If v and θ belong to set $\mathscr{L}$, then the deadzone non-linearity $\varphi(v)$ satisfies the following inequality, which is true for any matrix W in $\mathbb{S}_1^+$*

$$\varphi^\top(v)\mathrm{W}[\varphi(v) - \theta] \leq 0. \tag{21}$$

By taking into account the original system (7) and the identity (19), the following equivalent closed-loop representation is obtained

$$\begin{cases} x_{k+1} = \mathbb{A}x_k + \mathbb{A}_\mathrm{d}x_{k-d_k} - \mathrm{B}\varphi(v_k) + \mathrm{B}_\mathrm{q}q_k \\ v_k = \mathrm{K}x_k + \mathrm{K}_\mathrm{d}x_{k-d_k} \\ x_k = \phi_k, \ k \in [-d_\mathrm{M}, 0] \end{cases} \tag{22}$$

where $\mathbb{A} = \mathrm{A} + \mathrm{BK}$ and $\mathbb{A}_\mathrm{d} = \mathrm{A}_\mathrm{d} + \mathrm{BK}_\mathrm{d}$. This representation allows us to analyze the system stability using a combination of the Lyapunov functional (11) and the generalised sector condition provided in Lemma 4. Due to the saturating actuator, we need to analyse regional stability of (22), that is, we need to find a set of initial conditions ϕ_k for which the asymptotic stability of the closed loop is ensured. First of all, note that we can rewrite the LKF (11) in the following augmented form $\mathrm{V}_k = \overline{x}_k^\top \mathbb{P}\overline{x}_k$, with $\overline{x}_k = \begin{bmatrix} x_k^\top & x_{k-1}^\top & \cdots & x_{k-d_\mathrm{M}}^\top \end{bmatrix}^\top$ and:

$$\mathbb{P} = \begin{bmatrix} \mathbb{P}_0 & \mathbb{P}_{b_1} & 0 & \cdots & 0 & \cdots & 0 \\ \star & \mathbb{P}_{a_1} & \ddots & \ddots & \vdots & \ddots & \vdots \\ \star & \ddots & \ddots & \mathbb{P}_{b_{d_m}} & 0 & \cdots & 0 \\ \vdots & \ddots & \star & \mathbb{P}_{a_{d_m}} & \mathbb{P}_{d_1} & \ddots & \vdots \\ \star & \cdots & \star & \star & \mathbb{P}_{c_1} & \ddots & 0 \\ \vdots & \ddots & \vdots & \ddots & \ddots & \ddots & \mathbb{P}_{d_{d_\Delta}} \\ \star & \cdots & \star & \cdots & \star & \star & \mathbb{P}_{c_{d_\Delta}} \end{bmatrix},$$

where

$$\begin{aligned} \mathbb{P}_0 &= \mathrm{Q} + \mathrm{R}d_m^2 + \mathrm{R}_1 d_\Delta^2, \\ \mathbb{P}_{a_i} &= \mathrm{U} + 2\mathrm{R}_1 d_\Delta^2 + \mathrm{R}d_m(2d_m - 2i + 1), \\ \mathbb{P}_{b_i} &= -\mathrm{R}_1 d_\Delta^2 - \mathrm{R}d_m(d_m - i + 1), \\ \mathbb{P}_{c_j} &= \mathrm{U}_1 + \mathrm{R}_1 d_\Delta(2d_\Delta - 2j + 1), \\ \mathbb{P}_{d_j} &= -\mathrm{R}_1 d_\Delta(d_\Delta - j + 1), \end{aligned}$$

for $i \in [1, d_m]$ and $j \in [1, d_\Delta]$. Then, we define the set of initial conditions as $\mathbb{D}_\phi = \{\phi_k \in \mathbb{R}^{(d_\mathrm{M}+1)\times n}; \phi_k^\top \mathbb{P}\phi_k \leq \beta\}$, with $\beta > 0$.

4.2 | Stability in the saturated case

The following theorem provides a solution to Problem 1.

Theorem 2. *For given positive scalar σ, assume the existence of matrices $\mathrm{Q}, \mathrm{R}, \mathrm{U}, \mathrm{R}_1, \mathrm{U}_1$ in $\mathbb{S}_n^+$, matrices U_{12} in $\mathbb{R}^{n\times n}$, Z in $\mathbb{R}^{1\times n}$, W in $\mathbb{S}_1^+$, and positive scalars δ, μ such that*

$$\mathrm{T} = \begin{bmatrix} \mathrm{R}_1 & \mathrm{U}_{12} \\ \star & \mathrm{R}_1 \end{bmatrix} \succeq 0, \quad \Xi^{\perp^\top}\Phi\Xi^\perp \prec 0, \tag{23}$$

$$\Sigma = \begin{bmatrix} \mathrm{Q} & \mathrm{K}^\top\mathrm{W} - \mathrm{Z}^\top \\ \star & 2\mathrm{W}\sigma - \mu\left(\frac{\sigma}{\bar{u}}\right)^2 \end{bmatrix} \succeq 0, \tag{24}$$

$$\mu - \delta > 0, \tag{25}$$

with $\Xi^\perp = \begin{bmatrix} \mathbb{A} & 0 & 0 & \mathbb{A}_\mathrm{d} & -\mathrm{B} & \mathrm{B}_\mathrm{q} \\ & & \mathrm{I}_{4n+2} & & & \end{bmatrix}$ *and*

$$\Phi = \begin{bmatrix} \Upsilon & \begin{bmatrix} 0 & 0 \\ \mathrm{Z}^\top & 0 \\ 0 & 0 \\ 0 & 0 \\ \mathrm{K_d}^\top\mathrm{W} & 0 \end{bmatrix} \\ \star & \begin{bmatrix} -2\mathrm{W} & 0 \\ \star & -\mathrm{I} \end{bmatrix} \end{bmatrix},$$

where Υ *has been given in Theorem 1. Then*

1. *For any* $q \in \mathcal{Q}$ *and all* $\phi_k \in \mathbb{D}_\phi = \{\phi_k \in \mathbb{R}^{(d_\mathrm{M}+1)\times n}; \phi_k^\top \mathbb{P} \phi_k \leq \beta\}$, $\beta = \mu - \delta$, *the trajectories of (22) do not leave the ellipsoid given by* $\mathbb{D}_{\overline{x}} = \{\overline{x}_k \in \mathbb{R}^{(d_\mathrm{M}+1)\times n}; \overline{x}_k^\top \mathbb{P} \overline{x}_k \leq \mu\}$, *for all* $k > 0$.
2. *For* $q_k = 0$, *the set* $\mathbb{D}_{\overline{x}}$ *is a region of asymptotic stability of (22).*

Proof. First, consider an auxiliary matrix $\mathrm{G} \in \mathbb{R}^{1\times n}$ and application of Lemma 4 with $v = \mathrm{K}x_k + \mathrm{K_d}x_{k-d_k}$, $\theta = \mathrm{G}x_k + \mathrm{K_d}x_{k-d_k}$. If x_k belongs to the resulting set

$$\mathscr{L}(|\mathrm{K}-\mathrm{G}|, \overline{u}) = \{x \in \mathbb{R}^n; -\overline{u} \leq (\mathrm{K}-\mathrm{G})x \leq \overline{u}\}, \tag{26}$$

then the inequality:

$$-2\varphi^\top(v_k)\mathrm{W}\left[\varphi(v_k) - \mathrm{G}x_k - \mathrm{K_d}x_{k-d_k}\right] \geq 0 \tag{27}$$

is satisfied for some W in $\mathbb{S}_1^+$.

Consider also relation (24). Use the fact that

$$\left(\frac{\mu\sigma}{\bar{u}^2} - \mathrm{W}\right)^\top \frac{\mu^{-1}\bar{u}^2}{\sigma}\left(\frac{\mu\sigma}{\bar{u}^2} - \mathrm{W}\right) \succeq 0$$

to replace $2\mathrm{W}\sigma - \mu(\frac{\sigma}{\bar{u}})^2$ by $\mathrm{W}^\top\mu^{-1}\bar{u}^2\mathrm{W}$ in Σ. Then, pre- and post-multiply the obtained inequality by $\mathrm{diag}(\mathrm{I}, \mathrm{W}^{-1})^\top$ to obtain relation:

$$\begin{bmatrix} \mathrm{Q} & (\mathrm{K}-\mathrm{G})^\top \\ \star & \mu^{-1}\bar{u}^2 \end{bmatrix} \succeq 0$$

which ensures the inclusion of the ellipsoid $\varepsilon(\mathrm{Q}, \mu) = \{x_k \in \mathbb{R}^n; x_k^\top \mathrm{Q} x_k \leq \mu\}$ in the polyhedral set $\mathscr{L}$. Since $x_k^\top \mathrm{Q} x_k \leq \overline{x}_k^\top \mathbb{P} \overline{x}_k \leq \mu$, if $\phi_k \in \mathbb{D}_\phi$, then $x_k \in \varepsilon(\mathrm{Q}, \mu) \subset \mathscr{L}$, $\forall k > 0$, and the sector condition is effectively validated.

Now, consider relation (23). Replace $\mathrm{Z}^\top$ by $\mathrm{G}^\top\mathrm{W}$ in Φ and note that left and right multiplication of the resulting matrix by $\xi_k^\top$ and $\xi_k = \left[\gamma_k^\top \ \varphi(v_k)^\top \ q_k^\top\right]^\top$, respectively, leads to the expression

$$\xi_k^\top\Phi\xi_k = \gamma_k^\top\Upsilon\gamma_k - q_k^\top q_k - 2\varphi^\top(v_k)\mathrm{W}\left[\varphi(v_k) - \mathrm{G}x_k - \mathrm{K_d}x_{k-d_k}\right], \tag{28}$$

where the vector $\gamma_k = \left[x_{k+1}^\top \ x_k^\top \ x_{k-d_m}^\top \ x_{k-d_\mathrm{M}}^\top \ x_{k-d_k}^\top\right]^\top$ was first given in the proof of Theorem 1. From the proof of Theorem 1 and relation (21), we have that $\gamma_k^\top\Upsilon\gamma_k \geq \Delta\mathrm{V}_k$ and $-2\varphi^\top(v_k)\mathrm{W}\left[\varphi(v_k) - \mathrm{G}x_k - \mathrm{K_d}x_{k-d_k}\right] > 0$, respectively, leading to

$$\xi_k^\top\Phi\xi_k \geq \gamma_k^\top\Upsilon\gamma_k - q_k^\top q_k \geq \Delta\mathrm{V}_k - q_k^\top q_k. \tag{29}$$

Therefore, by guaranteeing that $\xi_k^\top\Phi\xi_k < 0$ we guarantee that $\Delta\mathrm{V}_k - q_k^\top q_k < 0$ for all $x_k \in \mathbb{D}_{\overline{x}}$, provided that $x_k \in \mathscr{L}$. Then by computing $\sum_{i=0}^k(\Delta\mathrm{V}_i - q_i^\top q_i) < 0$ it follows $\mathrm{V}_k - \mathrm{V}_0 - \sum_{i=0}^k q_i^\top q_i < 0$, $\forall k \geq 0$. In other words, this implies that

- $\mathrm{V}_k < \mathrm{V}_0 + \|q_k\|^2 \leq \beta + \delta = \mu$, for all $k \geq 0$, thus the trajectories of (22) remain bounded by the ellipsoid given by $\mathbb{D}_{\overline{x}} = \{\overline{x}_k \in \mathbb{R}^{(d_\mathrm{M}+1)\times n}; \overline{x}_k^\top \mathbb{P} \overline{x}_k \leq \mu\}$.
- If $q_k = 0$, $\forall k \geq \overline{k} \geq 0$, then $\Delta\mathrm{V}_k \leq 0$, ensuring that $x_k \to 0$, without leaving $\mathbb{D}_{\overline{x}}$, as $k \to \infty$.

From Finsler's Lemma, satisfaction of $\xi_k^\top\Phi\xi_k < 0$, $\forall\xi$ such that $\Xi\xi = 0$, $\xi \neq 0$, with $\Xi = \left[-\mathrm{I} \ \mathbb{A} \ 0 \ 0 \ \mathbb{A}_\mathrm{d} \ -\mathrm{B} \ \mathrm{B}_\mathrm{q}\right]$ (and therefore of $\Delta\mathrm{V}_k - q_k^\top q_k < 0$) along the trajectories of (22) is equivalent to the satisfaction of ${\Xi^\perp}^\top\Phi\Xi^\perp \prec 0$, where $\Xi^\perp$ is a basis for the null space of Ξ, thus leading to (23). This completes the proof of all the items in Theorem 2. □

Remark 4. Although the dimension of the matrix $\mathbb{P}$ can be high, specially for long delays, it does not lead to some numerical burden of the optimisation schemes since the matrix $\mathbb{P}$ is not a decision variable in Theorem 2. In fact, the matrix $\mathbb{P}$ is assembled with the LKF matrices $\{\mathrm{Q}, \mathrm{R}, \mathrm{R}_1, \mathrm{U}, \mathrm{U}_1\}$, which are the decision variables in the theorem. Furthermore, as introduced in Section 2.3, all the works dealing with the LKF approach to stability of saturated discrete-time delayed systems characterise the region of attraction by bounding some norm of the sequence of initial condition (see for example [37]). In this case, conservative operations are involved to find the scalar bound on the norm. No such conservatism is present in the case we utilise the matrix $\mathbb{P}$ since it is an augmentation of the LKF, which does not require any extra bounding.

Additionally, for open-loop stable systems, one may look for a condition ensuring the global stability of the closed-loop system.

Corollary 1. *Assume the existence of matrices* Q, R, U, R_1, U_1 *in* $\mathbb{S}_n^+$, *matrices* U_{12} *in* $\mathbb{R}^{n\times n}$ *and* $\mathbb{W}$ *in* $\mathbb{S}_1^+$ *such that* $\mathrm{T} \succeq 0$, $\Xi^{\perp\top}\Phi\Xi^{\perp} \prec 0$ *with* T, Ξ, *and* Φ *defined in Theorem 2 and* $\mathrm{Z}^\top = \mathrm{K}^\top\mathrm{W}$, *then*

1. *For* $q_k = 0$, *the whole state-space is a region of asymptotic stability of (22).*
2. *For any* $q \in \mathcal{Q}$, *and any initial condition* $\phi \in \mathbb{R}^{(d_\mathrm{M}+1)\times n}$, *the trajectories of (22) remain bounded as follows:*

$$\mathrm{V}_k \leq \mathrm{V}_0 + \delta, \forall k \geq 0.$$

Proof. Proof is straightforward by noting that (27) is satisfied for all $x_k \in \mathbb{R}^n$ when $\mathrm{G} = \mathrm{K}$. In this case, both relations (24) and (25) become pointless. □

4.3 | Computational Issues

Theorem 2 provides conditions to prove regional stability results for the closed-loop system along with a characterisation of the ellipsoidal region of stability and the energy-bounded disturbance that affects the system. By application of the presented convex conditions, different analysis results can be exploited. In the following, we present two particular cases of interest. First, we would like to find out the maximum energy bound (δ) on the external disturbance belonging to the set $\mathcal{Q}$ when the system is at equilibrium ($\overline{x}_0 = 0$). Secondly, we are interested in maximising, in some sense, the estimate of the region of attraction.

4.3.1 | Disturbance tolerance maximisation

In the case of $\overline{x}_0 = 0$, it follows that $\beta = 0$ and $\mu = \delta$, and we seek to maximise the system tolerance to disturbances, that is, we aim at maximising the energy bound on the set $\mathcal{Q}$. For given positive scalar σ, the following optimisation procedure should be applied:

$$\begin{cases} \max\limits_{\{\mathrm{Q},\mathrm{R},\mathrm{U},\mathrm{R}_1,\mathrm{U}_1,\mathrm{U}_{12},\mathrm{Z},\mathbb{W},\mu\}} & \mu \\ \text{subject to (23), (24).} \end{cases} \tag{30}$$

4.3.2 | Maximisation of the plant initial conditions set

Consider system (7) affected by a fixed level of disturbance, that is a fixed δ. In this case, one is interested in maximising the estimate on the region of attraction, that is the ellipsoid $\mathbb{D}_{\overline{x}}$. Many different criteria can be adopted, such as volume maximisation and maximisation of the ellipsoid semi-minor axis. In this work, we adopt the later criteria, which is equivalent to the minimisation of the biggest eigenvalue of the matrix $\mathbb{P}\mu^{-1}$. The length of the semi-minor axis of the ellipsoid is equal to the radius of the maximum ball inside the ellipsoidal region of stability, and can be a useful qualitative measurement of the region in order to relate it to both the DTC tuning parameter ρ and the size of the delay. A convex optimisation procedure to indirectly achieve this goal is to run the following optimisation problem

$$\begin{cases} \min\limits_{\{\mathrm{Q},\mathrm{R},\mathrm{U},\mathrm{R}_1,\mathrm{U}_1,\mathrm{U}_{12},\mathrm{Z},\mathbb{W},\mu\}} & \kappa_1\lambda - \kappa_2\mu \\ \text{subject to (23), (24), (25), } \mathbb{P} \prec \lambda \mathrm{I}_{(d_\mathrm{M}+1)\times n} \end{cases} \tag{31}$$

with κ_1 and κ_2 tuning weighting on λ and μ. The length of the semi-minor axis can then be computed by $\omega_b = \lambda_{\max}^{-1/2}$, where $\lambda_{\max}$ is the maximum eigenvalue of the matrix $\mathbb{P}\mu^{-1}$. In the case that no perturbation affects system (7), we have $\delta = 0$. Since, we can remove the last column as well as the last line of $\Xi^{\perp\top}\Phi\Xi^{\perp}$ in (23) while running optimisation problem (31).

Remark 5. Note that the initial condition for the open-loop plant (1) is characterised only by x_{p_0}. Although for the time-delay closed-loop system (7) we could choose to consider the past states as zero and consider the initial condition as the special case $\phi_k = \begin{bmatrix} x_0^\top & 0 & \cdots & 0 \end{bmatrix}^\top$, $x_0 = \begin{bmatrix} x_{p_0}^\top & x_{s_0}^\top & x_{f_0}^\top \end{bmatrix}^\top$, we chose to consider the more general case in this paper with the sequence ϕ_k so that the initial condition can be anything as long as it is inside the set $\mathbb{D}_\phi = \{\phi_k \in \mathbb{R}^{(d_\mathrm{M}+1)\times n}; \phi_k^\top \mathbb{P} \phi_k \leq \beta\}$.

5 | NUMERICAL EXAMPLES

5.1 | Case study 1

This first example is dedicated to understanding how the DTC tuning parameter ρ relates to the system robustness. Simulations are performed for the open-loop unstable process $G(s) = \frac{1}{4s-1}$, studied in [28]. This model represents the linearised dynamical behaviour of the output concentration of some chemical reactors around the unstable operation point.

As in [28], it is assumed that there exists a measurement delay due to the time needed by the concentration transducer to give the output variable, which can vary between 0.5 and 0.7 seconds. By considering a sampling time of 0.1 seconds we obtain the discrete-time process model (1) with $\mathrm{A}_p = 1.0253$, $\mathrm{B}_p = 0.1250$ and $\mathrm{C}_p = 0.2025$ and time-varying delay $5 \leq d_k \leq 7$.

Initially, we consider the DTC design from [16] with $d_n = 6$, $\rho = 0.90$, and desired closed-loop pole $\{0.92\}$, so that fast set-point regulation is achieved in the ideal case (no saturation and no time-varying delay).

To illustrate the closed-loop system time-response, Figure 2 shows simulation results for an initial condition $\phi_k = 0$ $\forall k \in [-d_\mathrm{M}, 0]$, and disturbance signal of energy $\delta = 27.3053$. Stability is guaranteed by means of Theorem 2 with $\sigma = 0.01$, using optimisation problem (30). In this case $\mu = \delta$. Three cases are plotted:

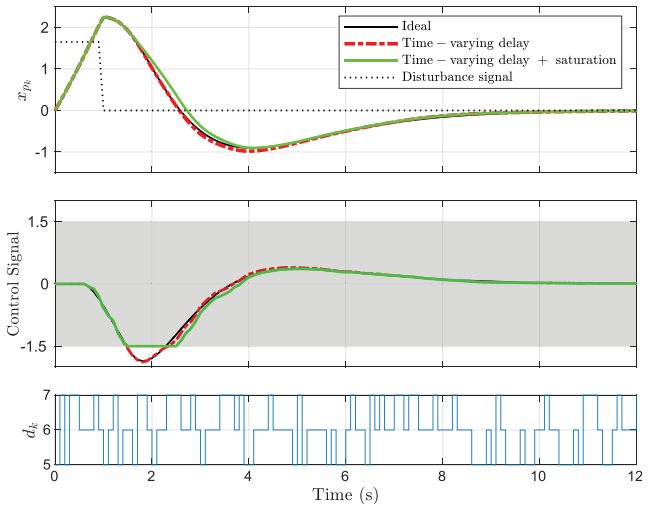

FIGURE 2 Case study 1 simulation results

TABLE 2 Case study 1- Admissible upper bound d_M for various values of ρ with $d_m = 5$ (unsaturated case)

ρ	0.89	0.91	0.93	0.95	0.97
d_M	9	10	12	15	18

- Ideal case, that is constant delay $d_k = d_n$ and no saturation $\overline{u} = \infty$.
- System with time-varying delay $5 \leq d_k \leq 7$ and no saturation, $\overline{u} = \infty$.
- System with both time-varying delay and saturation. In this case, for analysis purposes we consider $\overline{u} = 1.5$.

In the following sections, with the help from Theorems 1 and 2, and optimisation procedures (30), (31), we will give more comments on the simulations and how the values of ρ and $\overline{u}$ affect the system robustness and effectiveness.

5.1.1 | The unsaturated case

From Figure 2, it can be noted that the DTC controller is robust to the uncertainty introduced by the time-varying delay since the response is very close to the response of the ideal case. For an extended analysis, by means of Theorem 1, Table 2 provides the admissible upper bound d_M for various values of ρ with fixed $d_m = 5$.

From the DTC literature, it is well known that higher values of the robustness filter parameter ρ introduce more robustness to the system regarding uncertainties in the delay (in the constant case). This was also confirmed in the case of time-varying delays in [28]. As expected, Table 2 also illustrates this fact by showing that higher values of ρ allow for an increase in the admissible upper bound d_M on the delay. However, it is well-known in the DTC literature that higher values of ρ can also cause slower rejection of disturbances, which illustrates the trade-off between performance and robustness.

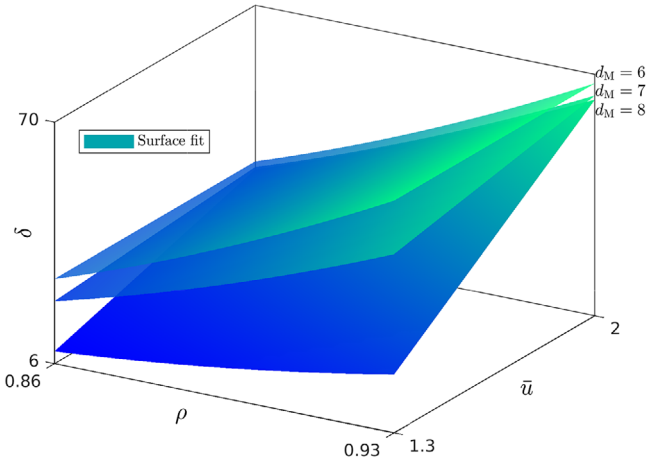

FIGURE 3 Relation between tuning parameter ρ, saturation limit $\overline{u}$, the maximum delay d_M (with $d_m = 5$), and the energy bound of the disturbance δ

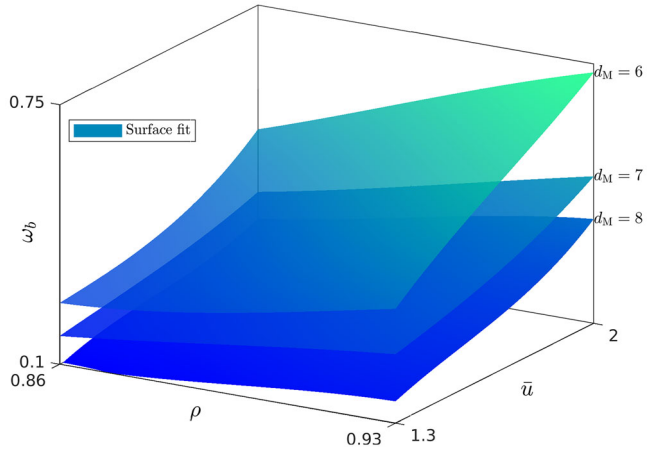

FIGURE 4 Relation between tuning parameter ρ, saturation limit $\overline{u}$, the maximum delay d_M (with $d_m = 5$), and the radius ω_b of the maximum ball inside $\mathbb{D}_{\overline{x}}$

5.1.2 | The saturated case

From Figure 2, note that although the control signal saturates at the beginning of the simulation, the controller is capable of bringing the system back to equilibrium in a nice manner.

In order to better understand the relation between tuning parameter ρ, the bound on the control signal $\overline{u}$, the plant delay and robustness of the DTC strategy, Figures 3 and 4 show multiple 3-dimensional surfaces for different values of the maximum delay d_M built by interpolating a data grid of $(\rho, \overline{u})$ values, in which the $z-axis$ represent δ and ω_b (the radius of the maximum ball inside $\mathbb{D}_{\overline{x}}$), respectively. Such results are obtained by means of optimisation problems (30) and (31) (in this case, with $\delta = 0$). One can observe that as ρ increases, the values of both ω_b and δ for which stability is guaranteed are increased. This

nicely illustrates that, as in the unsaturated LTI case, higher values of ρ improve the system overall robustness for systems with both time-varying delays and input saturation. Of course, as the control bound $\overline{u}$ is increased, the system also becomes suitable to deal with bigger initial conditions and disturbances of higher energy. Additionally, as the maximum delay d_{M} is increased, both the values of δ and ω_b decrease. This illustrates the bad impact of the time delay in the stability region, and also in the disturbance tolerance of the closed loop.

Finally, a special case worth of comment is that of known constant delay $d_m = d_{\mathrm{M}} = d_n = 5$. Using optimisation problems (30) and (31) with $\rho = 0.93$, $\overline{u} = 2$, we find significant increases in both ω_b and δ, being 1.0276 and 71.8202, respectively. This is due to the perfect delay compensation obtained by the predictor in this case. For consistency of the results, the desired closed-loop pole for the DTC design and the Theorem 2 constant σ were kept as $\{0.95\}$ and 0.05, respectively, throughout the simulations.

5.2 | Case study 2

Consider the NCS studied in [55]:

$$\dot{x}_p = \begin{bmatrix} -0.8 & -0.01 \\ 1 & 0.1 \end{bmatrix} x_p + \begin{bmatrix} 0.4 \\ 0.1 \end{bmatrix} u$$

By considering a sampling time of 0.5 seconds, an induced network time delay, and choosing the second state as output for the DTC design, we obtain the discrete-time model (1) with $\mathrm{A}_p = \begin{bmatrix} 0.6693 & -0.0042 \\ 0.4231 & 1.0501 \end{bmatrix}$, $\mathrm{B}_p = \begin{bmatrix} 0.1647 \\ 0.0960 \end{bmatrix}$, and $\mathrm{C}_p = \begin{bmatrix} 0 & 1 \end{bmatrix}$. In [55], the control law is given by $v_k = -\begin{bmatrix} 1.2625 & 1.2679 \end{bmatrix} x_{p_{k-d_k}}$, which guarantees closed-loop stability for a maximum induced delay of 1 second (or two samples), according to Theorem 4 of [55]. By using Theorem 1 of the work herein with $\mathbb{A} = \mathrm{A}_p$, $\mathbb{A}_{\mathrm{d}} = -\mathrm{B}_p \begin{bmatrix} 1.2625 & 1.2679 \end{bmatrix}$, we obtain that stability using the control law from [55] is guaranteed for a maximum delay in the range $1 \leq d_k \leq 3$. In the case of no delay, this control law would yield closed-loop poles $\{0.6950 + 0.0990i, 0.6950 - 0.0990i\}$. To design the DTC controller for this example, the desired closed-loop poles are chosen as $\{0.6950 + 0.0990i, 0.6950 - 0.0990i, 0.7\}$, and we initially set $\rho = 0.7$, which guarantees stability for the system by means of Theorem 1.

To illustrate the closed-loop system time-response, Figure 5 shows simulation results for an initial condition given by $x_{p_0} = \begin{bmatrix} 0.4919 \\ 0.4919 \end{bmatrix}$ and 0 in all other positions of ϕ_k. For illustration purposes, the response of the saturated closed loop is also plotted for the DTC with $\overline{u} = 1$. Stability in this case is guaranteed by means of Theorem 2 with $\sigma = 0.05$, using optimisation problem (31) with $\delta = 0, \kappa_1 = \kappa_2 = 1$, obtaining $\mu = 0.070866$. To enlarge the region of stability in the directions of the plant states a small modification in (31) was used with substitution of $\mathbb{P} \prec \lambda \mathrm{I}_{(d_{\mathrm{M}}+1)\times n}$ by $\begin{bmatrix} \mathrm{I}_{n_p} & 0 \end{bmatrix} \mathbb{P} \begin{bmatrix} \mathrm{I}_{n_p} & 0 \end{bmatrix}^{\top} \preceq \lambda \mathrm{I}_{n_p}$. Both strategies present similar performance, but the control signal of the DTC strategy is less aggressive, and the settling time for the first state is faster. It is important to recall, however, that opposed to the compared control law, the DTC strategy obtained the results by feedback of only one of the states.

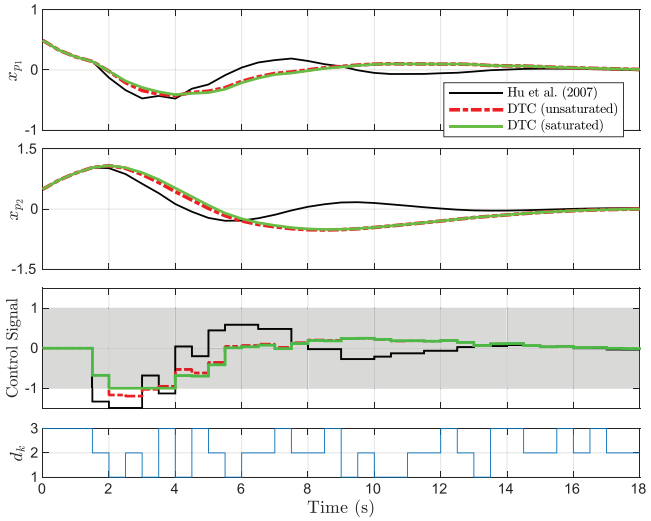

FIGURE 5 Case study 2 simulation results

TABLE 3 Case study 2- Admissible upper bound d_{M} for various values of ρ with $d_m = 1$

ρ	0.75	0.80	0.86	0.9
d_{M}	4	5	6	7

The main advantage of the DTC strategy is yet the possibility to deal with much bigger delays by simply increasing the value of ρ. To illustrate this, Table 3 shows the relation between the maximum delay d_{M} and ρ for this example, obtained by means of Theorem 1. As shown in the table, with the DTC, it is possible to guarantee stability for the system even for a time-varying delay in the range $1 \leq d_k \leq 7$ by only increasing ρ.

In conclusion, the use of the DTC is advantageous when there is no access to the measurement of the full state since the DTC is able to stabilise the system with only measurement of the output, and when it is desired to stabilise the system for longer delays in the network. On the other hand, the advantage with the classical state feedback law is its implementation simplicity, with closed-loop order $n = n_p = 2$, while the closed-loop order using the DTC is $n = 3n_p + d_n + 2 = 10$.

6 | EXPERIMENTAL RESULTS

This section shows practical results of the DTC structure, applied for temperature control of an in-house neonatal intensive care unit (NICU) prototype, depicted in Figure 6 [56]. The physical structure of the NICU prototype consists of two main parts: an acrylic dome in which the temperature should be controlled; and a reservoir right below the acrylic dome containing a

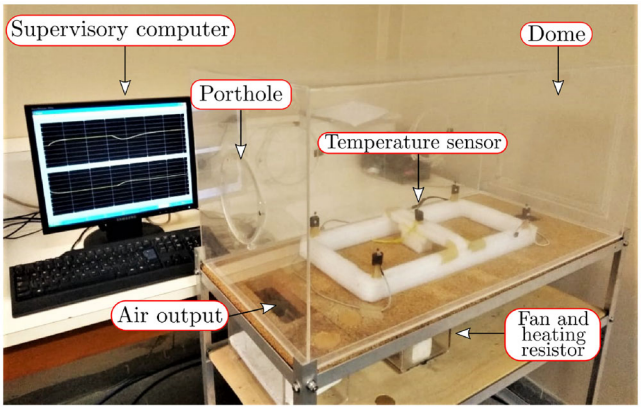

FIGURE 6 Picture of the NICU prototype

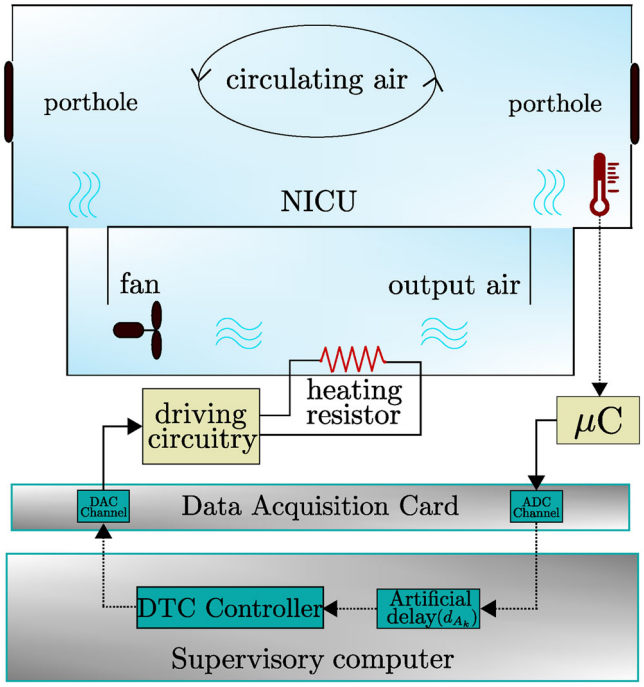

FIGURE 7 Experimental setup diagram of the NICU. Dashed lines refer to digital signals while solid ones refer to analogue signals

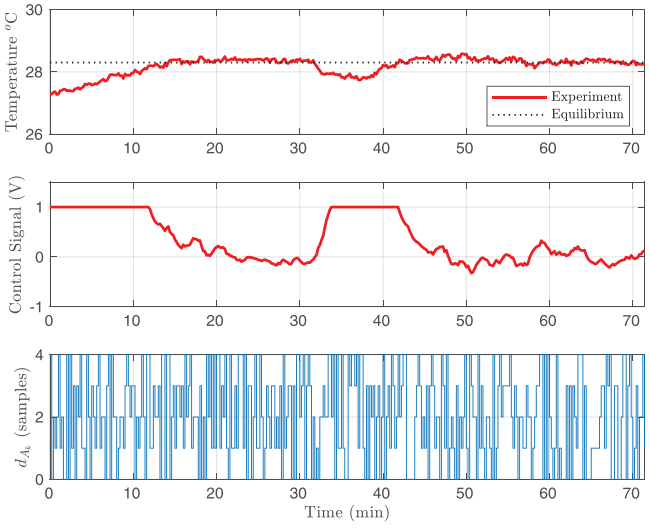

FIGURE 8 Experimental results: Temperature control of a NICU

heating resistor, and a fan with constant speed. These two environments are connected by two openings so that the heated air can circulate through the acrylic dome. The control variable is the electrical voltage applied, by means of a driving circuitry, to the terminals of the heating resistor, and is constrained in the range from 0 to 2 volts.

The driving circuitry is commanded by a supervisory computer through the digital-to-analog converter channel of a data acquisition card. In order to close the control loop, the temperature sensor inside the acrylic dome provides actual measurement to the supervisory computer by using a microcontroller (μC), which implements the communication protocols of the sensor and converts the digital data from the sensor to analogue voltage values, combined with the analog-to-digital converter channel of the same data acquisition card. The data acquisition card communicates with the supervisory computer through a USB cable.

In front of the acrylic dome, two portholes for manipulation of newborns are present which, when opened, disturb the temperature inside the dome due to the interaction with the external environment, which could be in much higher or lower temperature.

Using a step-test identification procedure [1], the plant model has been identified around an equilibrium point designated by the pair ($x_{p_{eq}} = 28.3^o$C, $u_{eq} = 1$ Volt) and is given by $P_n(s) = \frac{1.572e^{-1.17s}}{17.35s+1}$, where the time constant is given in minutes. Using a sampling time of 0.2 min, the discrete-time model is obtained as $P_n(z) = \frac{0.018017}{z-0.9885} z^{-6}$.

In order to experimentally validate the DTC ability to deal with both saturation and time-varying delays, we introduce an additional artificial measurement delay (d_{A_k}) which can vary between 0 and 4 samples and has been induced by software using a random number generator. Therefore, we obtain the discrete-time process model (1) with $A_p = 0.9885$, $B_p = 0.0180$, $C_p = 1$, time-varying delay $6 \leq d_k \leq 10$ and saturation level $\overline{u} = 1$. A detailed diagram depicting the incubator and the experimental setting is shown in Figure 7.

For the design of the DTC, the desired closed-loop pole is set as $\{0.94\}$, and the robustness filter $\mathcal{F}_r$ is tuned with $\rho = 0.93$ to achieve a good trade-off between system robustness and disturbance rejection speed. Global stability has been guaranteed by means of Corollary 1.

Experimental results are shown in Figure 8 for an initial temperature of 27.3 °C (one degree below the equilibrium temperature). It is important to note that even though the plant input became saturated during the first 12 min, the controller did not present windup issues and was able to go back to the equilibrium temperature of 28.3 °C. In order to further assess controller robustness, front portholes of the NICU were opened between $t = 31.4$ min and $t = 38.4$ min. The room temperature was at 19.9 °C during the experiment, which introduces a high level

of disturbance. Even though the control signal saturates again, such a disturbance was properly rejected and equilibrium was restored some time after.

Remark 6. The YALMIP toolbox [57] was used for solving the LMIs and optimisation problems throughout the paper. The obtained matrices $\{Q, R, U, R_1, U_1, U_{12}, Z, W\}$ for the two numerical examples and the experimental application can be consulted in [58].

7 | CONCLUSION

This work presented, for the first time, stability analysis of a dead-time compensator structure for input-saturated processes with output time-varying delays. The simulation case studies and the experiment for the control of temperature in a neonatal incubator effectively showed the good qualities of DTC structures dealing with the addressed type of process. The numerical examples were also used to show that the DTC tuning parameter ρ may adjust the classical trade-off between robustness and disturbance rejection performance. Since DTCs are a class of controller frequently used in practical applications, the developed analysis is of importance for the control of industrial dead-time processes.

On the theoretical side, the developed conditions were effective to properly analyse stability of the closed loop, and a potentially less conservative methodology for the definition of the set of initial conditions has been proposed, which can be used in works employing the LKF approach for stability analysis of discrete-time systems. Future work will address the stabilisation problem by developing a full state-space approach for the DTC which will allow LMI-based design of all the controller parameters, or of part of them. Also, we aim at using more elaborated LKFs in conjunction with less conservative inequalities. The analysis of other performance indexes as the H_∞ norm between the disturbance and the regulated output are also desired to be included. Finally, the extension to deal with LPV systems is also of great interest.

ACKNOWLEDGMENT

This study was financed in part by the Coordenação de Aperfeiçoamento de Pessoal de Nível Superior - Brasil (Capes) - Finance Code 001, and by ANR project HANDY 18-CE40-0010.

REFERENCES

1. Normey.Rico, J.E., Camacho, E.F.: Control of Dead-time Processes. Springer, Berlin (2007)
2. Fridman, E.: Introduction to Time-Delay Systems. Springer International Publishing, Berlin (2014)
3. Seuret, A., Gouaisbaut, F.: Wirtinger-based integral inequality: Application to time-delay systems. Automatica 49(9), 2860–2866 (2013)
4. Tarbouriech, S., et al.: Stability and Stabilization of Linear Systems with Saturating Actuators. Springer, London (2011)
5. Zaccarian, L., Teel, A.R.: Modern Anti-windup Synthesis: Control Augmentation for Actuator Saturation Princeton Series in Applied Mathematics. Princeton University Press, NJ (2011)
6. Wang, S., et al.: Saturated sliding mode control with limited magnitude and rate. IET Control Theory Appl. 12(10), 1075–1085 (2018)
7. Wang, Y., Ji, H.: Input-to-state stability-based adaptive control for spacecraft fly-around with input saturation. IET Control Theory Appl. 14(9), 1365–1374 (2020)
8. Hu, J. et al.: Non-fragile set-membership estimation for sensor-saturated memristive neural networks via weighted try-once-discard protocol. IET Control Theory Appl. 14(9), 1671–1680 (2020)
9. Zhang, X., Zhou, Z.: Integrated fault estimation and fault tolerant attitude control for rigid spacecraft with multiple actuator faults and saturation. IET Control Theory Appl. 13(10), 2365–2375 (2019)
10. Shen, Y., et al.: H∞ filtering for multi-rate multi-sensor systems with randomly occurring sensor saturations under the p-persistent csma protocol. IET Control Theory Appl. 14(10), 1255–1265 (2020)
11. Smith, O.J.M.: Closed control of loops with dead-time. Chem. Eng. Progress 53, 217–219 (1957)
12. Normey.Rico, J.E., Camacho, E.F.: Dead-time compensators: A survey. Control Eng. Pract. 16(4), 407–428 (2008)
13. García, P., Albertos, P.: Robust tuning of a generalized predictor-based controller for integrating and unstable systems with long time-delay. J. Process Control 23(8), 1205–1216 (2013)
14. Liu, T., et al.: New predictor and 2DOF control scheme for industrial processes with long time delay. IEEE Trans. Ind. Electron. 65(5), 4247–4256 (2018)
15. Sanz, R., et al.: A generalized smith predictor for unstable time-delay siso systems. ISA Trans. 72, 197–204 (2018)
16. Torrico, B.C., et al.: Tuning of a dead-time compensator focusing on industrial processes. ISA Trans. 83, 189–198 (2018)
17. Torrico, B.C., et al.: New simple approach for enhanced rejection of unknown disturbances in LTI systems with input delay. ISA Trans. 94, 316–325 (2019)
18. Sun, W., Fu, B.: Adaptive control of time-varying uncertain non-linear systems with input delay: a hamiltonian approach. IET Control Theory Appl. 10(15), 1844–1858 (2016)
19. Yang, R., Sun, L.: Finite-time robust control of a class of nonlinear time-delay systems via lyapunov functional method. J. Franklin Inst. 356(3), 1155–1176 (2019)
20. Rodríguez, C., et al.: Revisiting the simplified imc tuning rules for low-order controllers: Novel 2dof feedback controller. IET Control Theory Appl. 14(10), 1700–1710 (2020)
21. Yang, T.C.: Networked control system: a brief survey. IEE Proceedings - Control Theory and Appl. 153(4), 403–412 (2006)
22. Gupta, R.A., Chow, M.: Networked control system: Overview and research trends. IEEE Trans. Ind. Electron. 57(7), 2527–2535 (2010)
23. Zhang, D., et al.: Analysis and synthesis of networked control systems: A survey of recent advances and challenges. ISA Trans. 66, 376–392 (2017)
24. Sanz, R., et al.: Observation and stabilization of ltv systems with time-varying measurement delay. Automatica 103, 573–579 (2019)
25. Sanz, R., et al.: Robust predictive extended state observer for a class of nonlinear systems with time-varying input delay. Int. J. Control 0(0), 1–9 (2019)
26. Geng, X., et al.: Generalized predictor based active disturbance rejection control for non-minimum phase systems. ISA Trans. 87, 34–45 (2019)
27. Gonzalez, A., et al.: Gain-scheduled predictive extended state observer for time-varying delays systems with mismatched disturbances. ISA Trans. 84, 206–213 (2019)
28. Normey.Rico, J.E., et al.: Robust stability analysis of filtered smith predictor for time-varying delay processes. J. Process Control 22(10), 1975–1984 (2012)
29. Alves Lima, T., et al.: A practical solution for the control of time-delayed and delay-free systems with saturating actuators. European J. Control 51, 53–64 (2020)
30. Tarbouriech, S., Gomes da Silva Jr., J.M.: Synthesis of controllers for continuous-time delay systems with saturating controls via LMIs. IEEE Trans. Autom. Control 45(1), 105–111 (2000)
31. Fridman, E., et al.: Regional stabilization and h∞ control of time-delay systems with saturating actuators. Int. J. Robust Nonlinear Control 13(9), 885–907 (2003)

32. Gomes da Silva Jr., J.M., et al.: Anti-windup design for time-delay systems subject to input saturation an LMI-based approach. European J. Control 12(6), 622–634 (2006)
33. Gomes da Silva Jr., J.M., et al.: Non-rational dynamic output feedback for time-delay systems with saturating inputs. Int. J. Control 81(4), 557–570 (2008)
34. Chen, Y., et al.: Stabilization of neutral time-delay systems with actuator saturation via auxiliary time-delay feedback. Automatica 52, 242–247 (2015)
35. Chen, Y., et al.: Robust stabilization for uncertain saturated time-delay systems: A distributed-delay-dependent polytopic approach. IEEE Trans. Autom. Control 62(7), 3455–3460 (2017)
36. Seuret, A., et al.: Hierarchical estimation of the region of attraction for systems subject to a state delay and a saturated input. In: 2019 18th European Control Conference (ECC), 2019, pp. 2915–2920
37. Chen, Y., Fei, S.: Exponential stabilization for discrete-time time-delay systems with actuator saturation. In: Proceedings of the 33rd Chinese Control Conference, Nanjing, 2014, pp. 6130–6135
38. Naamane, K., et al.: Stabilization of discrete-time T-S fuzzy systems with saturating actuators. In: 2017 International Conference on Advanced Technologies for Signal and Image Processing (ATSIP), Fez, 2017, pp. 1–5
39. de Souza, C., et al.: ISS robust stabilization of state-delayed discrete-time systems with bounded delay variation and saturating actuators. IEEE Trans. Autom. Control 64(9), 3913–3919 (2019)
40. Zhang, B., et al.: Improved stability criterion and its applications in delayed controller design for discrete-time systems. Automatica 44(11), 2963–2967 (2008)
41. Shao, H., Han, Q.L.: New stability criteria for linear discrete-time systems with interval-like time-varying delays. IEEE Trans. Autom. Control 56(3), 619–625 (2011)
42. Liu, J., Zhang, J.: Note on stability of discrete-time time-varying delay systems. IET Control Theory Appl. 6(2), 335–339 (2012)
43. Seuret, A., et al.: Stability of discrete-time systems with time-varying delays via a novel summation inequality. IEEE Trans. Autom. Control 60(10), 2740–2745 (2015)
44. Hien, L.V., Trinh, H.: New finite-sum inequalities with applications to stability of discrete time-delay systems. Automatica 71(Supplement C), 197–201 (2016)
45. Zhang, X.M., et al.: An improved reciprocally convex inequality and an augmented lyapunov-krasovskii functional for stability of linear systems with time-varying delay. Automatica 84, 221–226 (2017)
46. Seuret, A., Gouaisbaut, F.: Stability of linear systems with time-varying delays using Bessel-Legendre inequalities. IEEE Trans. Autom. Control 63(1), 225–232 (2018)
47. Zhu, X.L., Yang, G.H.: Jensen inequality approach to stability analysis of discrete-time systems with time-varying delay. In: 2008 American Control Conference, Seattle, WA, 2008, pp. 1644–1649
48. Park, P., et al.: Reciprocally convex approach to stability of systems with time-varying delays. Automatica 47(1), 235–238 (2011)
49. de Oliveira, M.C., Skelton, R.E.: Stability tests for constrained linear systems. In: Moheimani, S.O.R., (ed.) Perspectives in robust control, pp. 241–257. Springer London, London (2001)
50. Nam, P.T., et al.: Discrete wirtinger-based inequality and its application. J. Franklin Inst. 352(5), 1893–1905 (2015)
51. Pandey, S., et al.: Comments on new finite-sum inequalities with applications to stability of discrete time-delay systems. Automatica 91, 320–321 (2018)
52. Kwon, O.M., et al.: Stability and stabilization for discrete-time systems with time-varying delays via augmented lyapunov-krasovskii functional. J. Franklin Inst. 350(3), 521–540 (2013)
53. Fridman, E.: A new lyapunov technique for robust control of systems with uncertain non-small delays. IMA J. Math. Control Inf. 23(2), 165–179 (2006)
54. Gomes da Silva Jr., J.M., Tarbouriech, S.: Antiwindup design with guaranteed regions of stability: An LMI-based approach. IEEE Trans. Autom. Control 50(1), 106–111 (2005)
55. Hu, L.S., et al.: Sampled-data control of networked linear control systems. Automatica 43(5), 903–911 (2007)
56. Pereira, R.D.O., et al.: Implementation and test of a new autotuning method for PID controllers of TITO processes. Control Eng. Pract. 58, 171–185 (2017)
57. Löfberg, J.Y.: A toolbox for modeling and optimization in matlab. In: Proceedings of the CACSD Conference, Taipei, Taiwan, (2004)
58. Alves Lima, T., et al.: Analysis and experimental application of a dead-time compensator for input saturated processes with output time-varying delays. Institution of Engineering and Technology. (2020) Supplementary material at https://hal.archives-ouvertes.fr/hal-02965943

How to cite this article: Alves Lima T, Tarbouriech S, Gouaisbaut F, et al. Analysis and experimental application of a dead-time compensator for input saturated processes with output time-varying delays. *IET Control Theory Appl.* 2021;15:580–593. https://doi.org/10.1049/cth2.12063